https://doi.org/10.5194/egusphere-2022-273
Preprint. Discussion started: 31 May 2022

Can soil spectroscopy contribute to soil organic carbon monitoring on agricultural soils?

Javier Reyes[1], Mareike Ließ[1]

[1]Helmholtz Centre for Environmental Research - UFZ, Soil System Science, Halle (Saale), Germany.

Correspondence to: Javier Reyes (javier.reyes@ufz.de); Mareike Ließ (mareike.liess@ufz.de)

Abstract. Carbon sequestration in soils under agricultural use can contribute to climate change mitigation. However, the spatial-temporal monitoring of soil organic carbon (SOC) requires more efficient data acquisition. The use of soil Vis-NIR spectroscopy is a promising research field in this context. However, the interpretation of the recorded spectral signal with regards to SOC is not trivial due to the complexity of the soil matrix, and factors affecting the measurements under field conditions. A model-building process is required to relate the spectral signal to the SOC content. For this study, spectral on-the-go proximal measurements and soil sampling were conducted on a long-term field experiment (LTE) located in the state of Saxony-Anhalt, Germany. SOC values ranged between 14-25 g kg-1 due to different fertilization treatments. Partial least squares regression (PLSR) models were built on behalf of spectral laboratory and field measurements conducted with two spectrometers and preprocessed by various methods. A data correction of the field data was done with three different approaches: linear transformation, piecewise direct standardization (PDS), and external parameter orthogonalization (EPO). The models were then thoroughly interpreted with regards to spectral wavelength importance using regression coefficients (RC) and variable importance in projection scores (VIP). The detailed wavelength importance analysis disclosed the challenge of using soil spectroscopy for SOC monitoring. The use of spectrometers with a differing spectral resolution for soil Vis-NIR measurements under varying soil conditions revealed shifts in wavelength importance. Still, some wavelengths related to SOC were extracted (560 nm, 1330 nm, 1400 nm, 1720 nm, and 1900 nm) by various preprocessing methods and were highly important in models trained on both, laboratory, and field measurements. Furthermore, we showed, that the correction of spectral field data with spectral laboratory measurements improved the predictive performance of the models built on behalf of the proximal on-the-go sensing measurements.

1 Introduction

Soil organic carbon (SOC) is one of the most studied soil properties among diverse disciplines such as agriculture, plant science, ecology, and environmental science. It is of particular interest in the study of agricultural systems as an indicator of soil quality. Furthermore, it plays an important role in the context of climate change mitigation. With appropriate agricultural soil management, CO_2 soil emissions can be mitigated and the soil carbon sequestration increased as these soils are far from their storage capacity (Lal, 2004; West and Marland, 2012). The initiative “4 per mile” launched at the Paris COP 21 Climate

https://doi.org/10.5194/egusphere-2022-273
Preprint. Discussion started: 31 May 2022

Change Agreement (UNFCCC, 2015), aims to increase the global SOC stocks by 0.4 percent per year through agricultural practices to mitigate the atmospheric CO_2 concentration derived from anthropogenic activities (Lal, 2016). The potential of reaching the desired SOC stocks should be assessed by considering the feasibility and effectiveness of management practices (Minasny et al., 2017; Poulton et al., 2018). For this reason, spatial-temporal monitoring of SOC in soils under agricultural use is needed.

Long-term field experiments (LTEs) provide a good insight to monitor changes in SOC stocks with regards to soil management, its temporal variability, and the balance under different treatments. LTEs have been established for more than a century to evaluate the effect of different agricultural management on soil and crop characteristics which can only be observed in the long term (Körschens, 2006). Grosse et al. (2020) and Grosse and Hierold (2019) provide an overview of German LTEs. They identified a total of 205 LTEs with a minimum duration of 20 years, of which 140 trials are still ongoing. 50 trials have a duration between 49-99 years and 3 trials have lasted more than 100 years. Most of the LTEs correspond to arable field crops (168) and most of them were established for fertilization experiments. However, repeated sampling and conventional laboratory measurements of SOC on all LTE plots are expensive in terms of manpower and analysis costs.

Striving toward more cost and time-efficient SOC data acquisition, the use of VIS-NIR (400-2500 nm) spectroscopy has increased over the last years (Soriano-Disla et al., 2014; Angelopoulou et al., 2020; Ahmadi et al., 2021). The SOC predictions in combination with spectral data are done through the model building by different approaches such as machine learning methods (Angelopoulou et al., 2020) and partial least squares regression (PLSR), with the latter being one of the most applied methods due to its capacity to address multicollinearity and achieve dimensionality reduction (Viscarra Rossel et al., 2006; Stenberg et al., 2010). The raw spectral data is affected by instrumental noise and baseline variations. Thus, it is necessary to apply preprocessing methods such as scatter-correction and spectral derivatives, although there is not a standardized procedure concerning soil spectra. Model interpretation and, hence the identification of SOC-specific wavelengths can be achieved through different approaches, some are intrinsically included in the PLSR model, i.e. regression coefficients, loading weights, explained variance, etc. (Sarathjith et al., 2016). The interpretation of the recorded signal information with regards to SOC is not trivial as spectral absorption features are caused by the stretching and bending of structural molecule groups which are embedded in a complex soil matrix. Due to the soil complexity, an overlap of spectral response from organic and minerals compounds is observed (Ladoni et al., 2010). Although fundamental features associated with SOC are found in the MID-Thermal range (2500-25000 nm), weak overtones and combinations of fundamental vibrations due to the bending and stretching of NH, OH, and CH groups dominate the VIS-NIR range (Reeves, 2010; Ladoni et al., 2010; Knox et al., 2015). Different examples of important wavelengths associated with SOC in the VIS range (400-700 nm) (Rossel et al., 2006; Brown et al., 2006; Daniel et al., 2004), and in the NIR range (700-2500 nm) (Dalal and Henry, 1986; Daniel et al., 2004; Sudduth and Hummel, 1991; Shephered and Walsh, 2002) were identified. It is known that some wavelengths will have more relevance in a regression model as they are associated with specific soil properties (Lee et al., 2009; Sarathjith et al., 2016).

Several factors affect spectral measurements. Steps included in the measurement protocol such as instrument type, instrument setup, replicate measurements, sample preparation, and internal standard impact the accuracy and precision of the obtained

https://doi.org/10.5194/egusphere-2022-273
Preprint. Discussion started: 31 May 2022

data (Pimstein et al., 2011; Gholizadeh et al., 2017). Ge et al. (2011) stated that while it has not been profoundly studied, multiple instruments/scanning environments can have a significant effect on the soil spectra, and, consequently, on the modeling. Ellinger et al. (2019) studied the uncertainty propagation of the spectral signal in PLSR models considering repetitions and preprocessing methods. While under laboratory conditions most aspects can be controlled or accounted for, field measurements pose additional challenges: On-the-go measurements do not allow for replicate measurements of the same sample. Additionally, the contact between soil and spectrometer might be lost while the spectrometer is pulled through the soil, and the spectra are recorded under varying soil moisture (Sudduth and Hummel, 1993; Boregki and Lee, 2006; Bricklemyers and Brown, 2010; Minasny et al., 2011; Biney et al., 2020). Other factors to consider are surface roughness, crop residuals and/or roots, incident light, soil texture, bulk density, and soil structure (Minasny et al., 2011; Bellon-Maurel and McBratney, 2011) which adds more disturbance effects to the spectral signal. To remove the effect of field conditions on the spectra, different methods such as direct standardization, piecewise direct standardization, external parameter orthogonalization, and orthogonal signal correction (Nawar et al., 2020) could be used when measurements obtained under laboratory conditions are available.

This study aims to evaluate the ability of soil spectroscopy obtained from proximal on-the-go measurements to predict SOC since this data could provide a valuable source for spatio-temporal monitoring of SOC variation at field scale. Two instruments with different spectral resolutions were used to collect data under laboratory and field (on-the-go below ground and site-specific above ground) conditions to evaluate if the prediction of on-the-go spectroscopy can be used for SOC monitoring, by maintaining an adequate performance compared with the controlled laboratory conditions. A data correction of field measurements to improve the predictive model performance for SOC estimation is done by using 3 different approaches and model interpretation with regards to wavelength importance in PLSR models is performed with two indices: regression coefficients (RC) and variable importance in projection scores (VIP), to analyze for consistency of important wavelengths associated with SOC from laboratory conditions to field measurements.

2 Methods

2.1 Study area

Data collection was conducted on the LTE site Static Fertilization Experiment in Bad Lauchstädt, Saxony-Anhalt, Germany (51°24' N, 11°53'E, 113 m a.s.l). The climate is characterized by an average total annual precipitation of 470-540 mm and an average mean temperature of 8.5-9.0°C. The soil was classified as Haplic Chernozem developed from loess (Altermann et al., 2005) according to the German soil classification system (Ad-hoc-AG Boden, 2005). Topsoil texture varies between highly clayey silt (Ut4) and highly silty clay (Tu4) according to the German soil survey system (Ad-hoc-AG Boden, 2005). The Static Fertilization Experiment was initialized in 1902 by Schneidewind and Gröbler and is about 4 ha in size (Merbach and Schulz, 2013). It has eight subfields (Fig. 1) and was initialized with a crop rotation of winter wheat – sugar beet – summer barley –

https://doi.org/10.5194/egusphere-2022-273
Preprint. Discussion started: 31 May 2022

potato. From 2015 onwards, sugar beet and potatoes were replaced by silage maize to reduce the workload. The crop rotation was initiated by different crops on adjacent fields so that always all crops are grown simultaneously on the experimental site. Subfield one is limed with 30 dt every four years in spring. Since 1926, legumes were added to the crop rotation on subfield eight every 7th and 8th year. Additionally, the overall 288 plots differ according to their mineral and organic fertilizer treatments. Farmyard manure is applied with 20 t ha^{-1} and 30 t ha^{-1}, respectively, to one-third of the area of each field while the remaining third is left without organic fertilizer. Mineral fertilizer is applied in different combinations of N, P, and K, including the comparison of different N fertilizer types during a certain period. Subfields four and five of the experimental site were adapted in 1978 to investigate additional fertilizer treatments concerning different amounts of N in combination with an adapted organic fertilizer treatment. More details are given in Körschens and Pfefferkorn (1998).

2.2 Soil organic carbon data

The soil samples were acquired at 50 locations, at 0-10 cm depth (Fig. 1) according to a stratified random sampling design. Strata for random sampling were obtained by grouping the LTE plots according to their similarity by k-means cluster analysis. The following archive data were used to characterize each LTE plot: planted crops, agricultural treatment factors, total C, total N, available P, available K, and pH. In the end, 10 plots were randomly selected from each of the resulting five clusters, making a total of 50 plots to be sampled. Subsequently, one sampling point was randomly selected from each of the 50 plots excluding plot margins. The soil samples were air-dried, sieved (2 mm), and ground before carbon measurements with dry combustion. Total carbon was measured using the high-end elemental analyser vario EL cube CN (Elementar Analysensysteme GmbH) with 3 replicates per sample. The carbonate content was also measured, but values resulted below the detection level. Therefore, the total carbon was considered organic carbon.

2.3 Spectral measurements

Spectral measurements were taken using two devices: ASD FieldSpec 4 Hi-Res by Malvern Panalytical and Veris® Vis–NIR spectrophotometer by Veris Technologies, Inc (hereinafter will be called ASD and Veris, respectively). The ASD measures the Vis-NIR range (350–2500 nm), with a Full-Width Half Maximum of 3 nm in the Vis and 10 nm in the NIR, and an output of 1 nm spectral resolution. The Veris has an Ocean Optics USB4000 instrument (300 to 1100 nm) and a Hamamatsu TG series mini-spectrometer (1100 to 2200 nm), resulting in an output spectral resolution of 4-6 nm.

Field measurements were done with the ASD after crop harvest in sunny and dry soil conditions in September 2018. The spectra were measured at the soil surface at each sampling point using a 50 cm x 50 cm frame pointing north. Spectra were recorded at 5 replicate measurements with 3 external and 25 internal scans leading to a total of 15 spectra per sampling point. Veris field measurements were done the year after soil sampling in September 2019 due to logistic reasons. Several transects were recorded covering the entire field, with a 2-3 m distance and a measurement depth of about 12 cm. The device is built in

https://doi.org/10.5194/egusphere-2022-273
Preprint. Discussion started: 31 May 2022

a shank pulled through the soil by a tractor; measurements are made through a sapphire window mounted on the bottom of the shank Approximately 20 spectra per second are acquired (Christy, 2008).

ASD and Veris laboratory measurements were made in air-dried and sieved (2 mm) samples. For these measurements, the Veris spectrometer was removed from the shank. Soil samples were divided into 3 subsamples and filled in Petri dishes. Each subsample was measured 3 times and rotated 90° to measure another 3 times resulting in 6 replicate measurements with 3 external scans each. Internally, the ASD was set to conduct 25 readings, the Veris conducted 20 readings for each scan. Laboratory measurements resulted in 18 spectra per sample.

2.4 Data preparation for model building

In this study, SOC and spectral measurements were averaged for each sampling location. For Veris and ASD laboratory measurements the 18 spectra per sample were averaged. For ASD field measurements the recorded 15 spectra per sampling point were averaged. From the Veris on-the-go field measurements, the 10 spectra nearest to each sampling point within the same LTE plot were averaged. The ASD spectra were affected by steps in reflectance values at the splice of the three sensors at 1000 and 1800 nm of the spectroradiometer. Consequently, an ASD splice correction was implemented using the spectacles R-package (Roudier, 2020) which is based on the method described by Beal and Eamon (2010). For the Veris, the spectral range between 1000 to 1100 nm was removed due to the noise generated at the beginning and end of the two spectrometers. The spectral range selected for the model building was 400-2200 nm to allow for comparison between both devices, and to remove the beginning and end of the spectral range due to noise. Outliers were removed from the spectral measurements assigned to each sampling point by the adjusted quantile function in the mvoutlier package (Filzmoser and Gschwandtner, 2018). In the case of the Veris on-the-go data, the outlier removal was done before the selection of the 10 nearest spectra.

The aim of data preprocessing is to reduce the scattering effects that influence the spectral signal. There is not a unique recommended preprocessing method to predict SOC. Therefore, different techniques were applied to observe the influence on model prediction and wavelength importance. The four applied combinations were: Savitzky–Golay (SG; Savitzky and Golay, 1964), Savitzky–Golay + continuum removal (SGCR; Clark and Roush, 1998), gap segment algorithm (gapDer; Hopkins, 2003), and multiplicative scatter correction (MSC; Martens et al., 1983). Details are presented in Table 1. SG, SGCR, and gapDer were obtained using the prospectr R-package (Stevens and Ramirez Lopez, 2014) and the MSC by using the pls R-package (Mevik et al., 2019). A total of 16 datasets for the model building were obtained from a combination of the average spectral measurements using the two devices in the field and laboratory, and four different preprocessing techniques.

2.5 Model building and evaluation

PLSR (Wold et al., 2001) was applied to build regression models for SOC prediction. Model training, tuning, and evaluation were performed with a stratified 5-fold nested cross-validation (see details in Ellinger et al., 2019). To avoid spatial correlation between test and training data, neighboring samples within 8 m distance were grouped in the same fold. Model evaluation was done with 5 repetitions. Thus, 25 PLSR models were obtained for each dataset. Equal data subdivisions were used to compare

https://doi.org/10.5194/egusphere-2022-273
Preprint. Discussion started: 31 May 2022

different preprocessing methods, spectrometers, and field versus laboratory measurements. Root mean square error (RMSE) and R-squared were used as an error metric of model performance. Also, the Concordance Correlation Coefficient (Lin, 1989) is presented in predicted versus observed values plots.

2.6 Field data correction

To improve the model performance of ASD and Veris field spectral data, three approaches were used for correction: linear transformation, piecewise direct standardization (PDS), and external parameter orthogonalization (EPO). The linear transformation was done by using a linear regression between the field and laboratory data of the average spectral value at each sampling location for each wavelength. The PDS algorithm (Wang et al., 1991) is a common method to relate each wavelength of a master spectrum with those of a secondary spectrum (laboratory and field in our case). The optimal parameters required to apply PDS are the PLSR number of components and the size of the wavelength window. This study considered a number of components of 1 to 10 and a windows size of 1 to 20 for parameter tuning. The EPO (Roger et al., 2003) uses the projection of the primary and secondary data into an orthogonal space. The EPO algorithm components and the procedure for its calculation are described by Minasny et al. (2011). It requires the determination of the number of EPO components. In our study, 1 to 10 EPO components were tested. To select the respective parameters for each data correction approach, nested cross-validation was applied following the same subdivision (external and internal validation) used for the PLSR model building.

2.7 Wavelength importance

Two indices were used to evaluate the wavelength importance in the PLSR models: RC and VIP. These indices can be obtained from the PLSR output and used for variable identification (Mehmood et al., 2012). The RC are the coefficients associated with each wavelength to predict the response variables, and they are expected to have higher values (in absolute magnitude) when variables are important to the model prediction. The VIP scores (Wold et al., 1993) are calculated as the weighted sum of squares of the PLSR weights, which consider the amount of explained variance in each extracted latent variable. A common criterion used for VIP variable selection is to keep wavelengths with scores above 1 (Farres et al., 2015). The equation is defined as:

$$VIP_j = \sqrt{\frac{p \sum_{a=1}^{A} [w_{aj}/\|w_a\|^2]}{\sum_{a=1}^{A} SS_a}} \quad (1)$$

where p is the total number of variables, SS_a is the sum of squares explained by the a^{th} PLSR component. Hence, the weights w_j are a measure of the contribution of each variable according to the variance explained by each PLSR component where $w_{aj}/\|w_a\|^2$ represents the loading weight (w_a) importance of the j^{th} variable. Meanwhile, the RC were directly extracted from an object created using the pls package, the VIP were calculated by using the plsVarSel R-package (Mehmood et al., 2012). To compare the wavelength importance between different spectrometers and measurement conditions, local maxima and minima were identified for RC and the local maxima values for VIP, with a window width span of 100 nm for RC and 50 nm for VIP.

https://doi.org/10.5194/egusphere-2022-273
Preprint. Discussion started: 31 May 2022

This resulted in a lower number of wavelengths for the Veris data due to the comparatively lower spectral resolution. The plots of local peaks were done using the ggplot2 R-package (Wickham, 2016).

3 Results

3.1 Performance metrics

The measured SOC content has a mean value of 19.6 g $kg^{-1}$and a range between 14-25 g kg^{-1}, showing a range of SOC values derived from the different fertilization treatments. Figure 2 presents the RMSE and R-squared boxplots from the five cross-validation repetitions for each dataset. For both devices, models built on behalf of the laboratory measurements resulted in a better predictive accuracy (Fig. 2) and a lower dispersion with a higher concordance correlation coefficient in the 1:1 plots (Fig. 3) in comparison with the field measurements. These results show the expected performance decline from ASD laboratory – Veris laboratory – ASD field – Veris field, even though the model performance of the Veris field data still shows adequate accuracy. The best model for each subgroup was: ASD laboratory–MSC (R^2=0.9, RMSE=0.9 g kg^{-1}), ASD field–MSC (R^2=0.77, RMSE=1.4 g kg^{-1}), Veris laboratory–gapDer (R^2=0.86, RMSE=1.1 g kg^{-1}), and Veris field–gapDer (R^2=0.7, RMSE=1.6 g kg^{-1}), showing that the best preprocessing method changed with the device but was maintained between laboratory and field when using the same spectrometer.

3.2 Corrected field data

To improve SOC estimation of models using field measurements with both ASD and Veris, corrections were done based on their corresponding laboratory data using 3 approaches: linear transformation, PDS, and EPO. The optimal parameter values for PDS and EPO are presented in Table 2. It can be observed that the optimal parameter values of Veris datasets for model building are lower compared with ASD for both, the PDS and EPO algorithms.

The predictive accuracy on behalf of the field data was improved for both, Veris and ASD data, (Fig. 4), although, it was not equally effective among the preprocessing methods. In general, EPO was the best approach when comparing the different preprocessing methods with exception of SGCR where the best results were obtained with the linear transformation. Meanwhile, the performance of PDS was generally below the other two approaches. Fig. 5 displays the respective scatter plots; the corrected data tend to be less dispersed and their concordance correlation coefficient is higher compared to the original field data. Nevertheless, even after correction, the predictive performance of the models trained on behalf of the corrected field data was still below that of the models trained with the laboratory data. By considering the highest improvement of the data correction in all cases, the comparison of the wavelength importance presented next is based on the spectrally corrected field data using EPO for SG, gapDer, and MSC, and linear transformation for SGCR preprocessing methods.

3.3 Wavelength importance

https://doi.org/10.5194/egusphere-2022-273
Preprint. Discussion started: 31 May 2022

Boxplots of the tuned number of PLSR components corresponding to the 25 models built for each of the 16 datasets are presented in Fig. 6. The median value of the number of components was 15 or lower, and the variance of values for each of the 16 datasets differed according to the spectrometer, measurement condition, and preprocessing technique. In general, the models built with ASD and Veris laboratory data presented a lower dispersion compared with the respective models derived from field data. This corresponds to lesser disturbance effects, and, therefore, explains their better accuracy. Models derived after preprocessing with gapDer tend to have fewer components compared to the other preprocessing methods, which could be caused by the lower number of resulting variables when gapDer is applied to the raw data.

Figure 7 shows the RC values, and Fig. 8 the VIP values that correspond to the 25 models (repeated cross-validation) for each of the 16 datasets. When comparing devices, the absolute RC values were lower for models built with ASD laboratory data compared to those of the models built with the Veris laboratory data (Fig. 7A) and increased with the decline in the model accuracy presented in Fig. 2. The magnitude of the RC values for the field data was lower for SG, gapDer and MSC (corrected by using the EPO algorithm) compared to their corresponding laboratory data. The dispersion from the median value is generally low, although it is higher in the case of models built from Veris laboratory and field data using gapDer. The fluctuation of RC values makes it difficult to compare important wavelengths among the datasets. i.e. identify wavelengths that are important for SOC prediction regardless of the measurement condition, device, and preprocessing method. This holds especially true for the models obtained from ASD data, where more wavelengths were considered for the model building due to the higher spectral resolution. In contrast, VIP values are standardized; thus, their magnitude is comparable among datasets and presents low dispersion in all cases. The pattern of VIP values was similar in some cases, particularly, between models built from ASD laboratory and field data using the same preprocessing method.

To facilitate the identification of wavelengths that relate to SOC and are, therefore, important independent of measurement condition, device, and preprocessing method, local peaks were identified for the median RC and VIP values (Fig. 9 and 10). Table 2 presents the peak matches of VIP local maxima between the models obtained using ASD laboratory data with MSC preprocessing (best model performance) and those from the models built on behalf of the other datasets. Due to differences in spectral resolution, the search range of peak matches was different for ASD (±10 nm) and Veris (±20 nm) datasets. For the RC local maxima and minima (Fig. 9), several peaks were concentrated in the NIR range independent of the device or preprocessing method, and in some cases, there is a match in the local peaks between devices and methods, but the sign is flipped. Regarding VIP, some noticeable peaks were around 1400 and 1900 nm, and others in the range of 1900-2200 nm.

The local peaks of VIP scores with the data of best model performance (ASD laboratory using MSC), presented most matches with ASD laboratory data using SG preprocessing (11 matches), fewer matches with gapDer (7 matches), and least with SGCR (6 matches) following the order of model accuracy. Regarding the ASD field data, SG also presented 11 matches, followed by MSC (10 matches), SGCR (6 matches), and gapDer (4 matches). Concerning the comparison of Veris laboratory and field data with the best model, fewer matches were observed, Veris laboratory data presented most matches (9) with MSC preprocessing and 6-7 for all but the gapDer preprocessing which resulted in only 3 matches.

https://doi.org/10.5194/egusphere-2022-273
Preprint. Discussion started: 31 May 2022

4 DISCUSSION

4.1 Model performance

The RMSE of the models is comparable to other studies when using ASD (Jiang et al., 2016, Liu et al., 2018) and Veris (Ellinger et al., 2019) under laboratory conditions; and has better accuracy than the results observed by Christy (2008) with Veris on silty soils under different fields, and ASD field measurements reported by Nocita et al. (2012) and Denis et al., (2014); both under sandy-loam and clay soils. The lower accuracy of the models using field measurements is likely due to factors such as varying soil moisture, illumination, and surface roughness (Viscarra Rossel et al., 2009; Jiang et al., 2016). This is particularly evident with soil moisture, where studies have obtained better performance under dry conditions (Minasny et al., 2011; Rienzi et al., 2014). The difference in predictive model performance between ASD field and Veris field data is caused not only by the spectral resolution but also by the device-dependent characteristics in data acquisition. The Veris field data were collected on-the-go below ground. Accordingly, for model training to relate the spectral information to SOC, the average of spectral measurements close to the respective soil sampling location was derived. While the top centimeter was very dry during measurement, there, was a notably higher soil moisture content at 12 cm depth. Additionally, in the on-the-go measurements, the soil contact of the sensor is affected during the movement due to the presence of clods, and stones. Thus, the Veris field spectral measurements are affected by more disturbance effects compared to the site-specific above-ground ASD measurements. Models obtained from the ASD laboratory data presented better performance compared with the Veris laboratory data displaying the mere effect of the inbuilt sensors and the lower spectral resolution. The soil spectral signal tends to have similar patterns, thus small changes in the slope of the continuous data are better observed with the higher resolution of the ASD. Regarding differences among preprocessing techniques, MSC shows better results with models derived from ASD data, and gapDer with models derived from Veris data. SG consistently presented good performance in each device and preprocessing technique. MSC and SG are widely used (Rinnan et al., 2009; Chen et al., 2013). MSC is a scatter-correction technique centered on reducing physical variability, thus, facilitating the modeling of soil chemical effects. SG is a spectral-derivative that removes multiplicative and additive effects (Dotto et al., 2018). In the case of gapDer, it creates datasets with the lowest number of wavelengths due to the size of the smoothing window, resulting in a lower number of resulting variables.

4.2 Wavelength importance

Differences in magnitude and sign of RC were identified, a finding which has also been reported by Ge et al. (2011) when using different instruments. It could be caused by models highly dependent on the instrument and scanning environment, hampering the transferability of models using different devices. The lower number of matching wavelength peaks in the models built on behalf of the Veris data compared to the best model trained with ASD data was expected due to the lower information content of the spectra (lower spectral resolution). From the identified wavelengths that relate to SOC independent of the measurement condition, device and preprocessing, the wavelengths peaks around 1400 and 1900 are also related to other soil

https://doi.org/10.5194/egusphere-2022-273
Preprint. Discussion started: 31 May 2022

properties, particularly the stretching and bending of the O-H bonds of free water (Conforti et al., 2018). Regarding the importance of these wavelengths, Kawamura et al. (2021) suggested that the retained water of air-dried soils influences SOC predictions because water retention increases with organic matter. Other high peaks in the range of 1900-2200 nm could be associated with the overtones and combination bands from CH compounds. More similarities in the local peaks were identified with VIP compared to RC. VIP demonstrated to be a good method to identify wavelength importance from local peaks, its usefulness has also been reported in other studies concerning SOC prediction (Viscarra Rossel et al, 2008; Jiang et al., 2016; Kawamura et al., 2017). In general, differences in wavelength importance were observed depending on the measurement condition, device, and preprocessing techniques, although with some concurrences at specific local peaks. It has to be noticed that both RC and VIP values are likely to change depending on the selected number of components in the PLSR (Fig. 2) which in turn also depends on the respective preprocessing method and spectral resolution of the recorded data.

Several of the wavelengths considered important for SOC prediction in both RC and VIP were found in the NIR range, agreeing with results reported by Peng et al. (2014) and Wang and Pan (2016), who used successive projections algorithm and VIP scores respectively. These results could be attributed to a stronger influence of CH bands, and also water content in the case of ASD and Veris in the field, as it is observed on the peaks of RC values around 1400 nm and 1900 nm in both cases (Fig. 9B and 9D). A notorious peak around 950-1000 nm of VIP values in the case of the Veris field datasets (Fig. 10D), could be attributed to soil water, although some wavelengths in this range were also identified as important for SOC in other studies (Lee et al., 2009; Vasques et al., 2009). In contrast to our findings, other studies report a dominance of important wavelengths in the VIS range (Yang et al., 2012; Colombo et al., 2014). These differences could be attributed to the soil particularities, measurement settings (e.g. spectrometer, protocols), and preprocessing techniques since SOC influences a wide range of wavelengths in the Vis-NIR region. In line with our findings, Lee et al. (2009) evaluated the performance of the 3 independent spectrometers and their corresponding wavelength ranges included in an ASD field spectrometer and reported the 1800-2500 nm range to result in better predictive performance for SOC.

When comparing different preprocessing methods, patterns were more similar in the models derived from ASD measurements compared with those derived from Veris data. This goes in line with our previous findings: The models built with differently preprocessed ASD laboratory data presented similar model performance (Fig. 3) and low variation in the number of components (Fig. 6). Preprocessing techniques can significantly affect both, predictive performance (Dotto et al., 2018) and wavelength importance (Peng et al., 2014).

The Veris data preprocessed with gapDer had resulted in the best models for both, laboratory and field data. This could be caused due to the total number of local peaks being lower with gapDer compared with the other preprocessing methods, and by differences in resolution, while it is more similar when the same preprocessing method is used (MSC). Matching patterns of important wavelengths independent of the preprocessing method are promising. For it implies that these wavelengths are ultimately reflecting the response of the soil characteristics rather than being caused by the data transformation. Some of the most frequent important wavelengths independent of the devices used in the field and laboratory and the preprocessing methods

https://doi.org/10.5194/egusphere-2022-273
Preprint. Discussion started: 31 May 2022

are similar to those reported by other studies: 560 nm (Brown et al., 2006), 1330 nm (Kooistra et al., 2003), 1400 nm, and 1900 nm (Conforti et al., 2018), and 1720 nm (Sudduth and Hummel, 1991).

4.3 Spectral correction of the field measurements

The spectral correction of the field data on behalf of the laboratory data improved the model performance, which could help to obtain better information under field conditions. Concerning the parameters for PDS and EPO, lower values were determined for Veris compared to ASD which could be expected due to the lower spectral resolution of the Veris data. The best results were obtained by using the EPO method, meanwhile, linear transformation showed better results than the PDS algorithm when comparing several datasets, indicating that is also a valid alternative for data correction. Nawar et al. (2020) also found the best performance with EPO compared to PDS when using a cubist model for SOC prediction, which they related to the capacity of the EPO algorithm to remove the effect of soil moisture in the spectral signal. Nevertheless, the different data correction approaches satisfactorily improved SOC prediction on behalf of the spectral field data. This is of particular importance in the context of spatially continuous SOC monitoring, which has to be conducted under field conditions. But, while spectral data correction with site-specific spectral soil measurements is commonly applied to remote sensing data (Stevens et al., 2008; Peng et al., 2015; Jiang et al., 2016; Crucil et al., 2019), the spectral correction of proximal-sensed spectral field measurements with spectral laboratory data is less commonly used. Only few examples related to SOC prediction are found that employ PDS (e.g. Ji et al., 2015a, Nawar et al., 2020) and EPO (Ji et al., 2015b, Nawar et al., 2020, Wijewardane et al., 2020). Applications related to on-the-go spectral recording are hardly available (e.g. Nawar et al., 2020). Our results indicate that spectral correction with laboratory data is a promising approach to be considered while using on-the-go spectral field measurements for SOC monitoring.

Despite the loss of accuracy in SOC estimation using field measurements, it is possible to identify similarities in the wavelength importance between models from field and laboratory data, including the Veris on-the-go field measurements, which had been sampled at different depth and date, indicating that even with additional uncertainties the models can show relevant wavelengths associated with SOC. This consistency of the models is not only important for SOC monitoring with on-the-go proximal sensing but also when combining data from different devices, and measurement protocols to build universal models of soil spectroscopy and establish it as a measurement method. The collection of worldwide data in large spectral libraries follows this line of thought (e.g. Roudier et al., 2017; Liu et al., 2018; Seidel et al., 2019).

5 Conclusions

The PLSR models presented good performance to predict SOC from on-the-go field measurements to allow for spatial-temporal SOC monitoring. We demonstrated that spectral correction of the sensor's field data with its laboratory data resulted in an improvement in predictive model performance, particularly by using the EPO algorithm. Hence, we consider spectral

https://doi.org/10.5194/egusphere-2022-273
Preprint. Discussion started: 31 May 2022

correction not only important while using remotely sensed spectral data (as commonly applied), but also while using proximally sensed data for spatial-temporal SOC monitoring under field conditions and suggest including it in any protocol for spectral field measurements.

The detailed model insight and interpretation of important wavelengths with regards to SOC detected matches in important wavelengths independent of the sensor and measurement conditions showing the capability of the models to detect important wavelengths even when the measurement conditions and acquisition methods differ. This consistency justifies the application of the methodology due to the physical meaning of the SOC-spectra relationship. Nevertheless, this detailed analysis also disclosed the challenge of using soil spectroscopy for SOC monitoring. Differences in wavelength importance were observed depending on the measurement instruments, and preprocessing methods, which added complexity to identifying relevant wavelengths. This is also a key aspect to consider when building large spectral libraries to generate universal spectral models to establish soil spectroscopy as a measurement method for SOC. Further work is needed to explain the differences between sensors and measurement conditions to develop best-practice protocols and standards for soil spectroscopy.

Author contribution

Spectral measurements, programming, and data analysis (JR), conceptual design, programming framework, and scientific embedding (ML), manuscript writing (JR, ML).

Competing interests

The authors declare that they have no conflict of interest.

Acknowledgments

This publication is part of the SOCmonit project – Monitoring of soil organic carbon with remote and proximal soil sensing methods. The project is supported by funds of the Federal Ministry of Food and Agriculture (BMEL) based on a decision of the Parliament of the Federal Republic of Germany via the Federal Office for Agriculture and Food (BLE) under the innovation support programme.

https://doi.org/10.5194/egusphere-2022-273
Preprint. Discussion started: 31 May 2022

References

Angelopoulou, T., Balafoutis, A., Zalidis, G., and Bochtis, D: From Laboratory to Proximal Sensing Spectroscopy for Soil Organic Carbon Estimation—A Review, Sustainability, 12(2), 443, https://doi.org/10.3390/su12020443, 2020.

Ad-hoc-Arbeitsgruppe Boden: Bodenkundliche Kartieranleitung, 5. Aufl., Bundesanstalt für Geowissenschaften und Rohstoffe in Zusammenarbeit mit den Staatlichen Geologischen Diensten, Hannover, Germany, 2005.

Ahmadi, A., Emami, M., Daccache, A., and He, L.: Soil Properties Prediction for Precision Agriculture Using Visible and Near-Infrared Spectroscopy: A Systematic Review and Meta-Analysis. Agronomy, 11(3), 433, https://doi.org/10.3390/agronomy11030433, 2021

Altermann, M., Rinklebe, J., Merbach, I., Körschens, M., Langer, U., and Hofmann, B. (2005). Chernozem – Soil of the Year 2005. J. Plant Nutr. Soil Sc., 168, 725-740, https://doi.org/10.1002/jpln.200521814

Beal, D., and, Eamon, M., (1996). Dynamic, Parabolic Linear Transformations of 'Stepped' Radiometric Data. Analytical Spectral Devices Inc., Boulder: CO.

Bellon-Maurel, V., and McBratney, A.: Near-infrared (NIR) and mid-infrared (MIR) spectroscopic techniques for assessing the amount of carbon stock in soils – Critical review and research perspectives. Soil Biology and Biochemistry, 43, 1398-1410, https://doi.org/10.1016/j.soilbio.2011.02.019, 2011.

Bogrekci, I., and Lee, W.S: Effects of soil moisture content on absorbance spectra of sandy soils in sensing phosphorus concentrations using UV–VIS–NIR spectroscopy. Trans ASABE, 49, 1175-1180, https://doi.org/10.13031/2013.21717, 2006.

Bricklemyer, R, and Brown, D.: On-the-go VisNIR: Potential and limitations for mapping soil clay and organic carbon. Computers and Electronics in Agriculture 70, 209-216, https://doi.org/10.1016/j.compag.2009.10.006, 2010.

Brown, D. J., Shepherd, K. D., Walsh, M. G., Dewayne Mays, M., and Reinsch, T. G.: Global soil characterization with VNIR diffuse reflectance spectroscopy, Geoderma, 132, 273-290, https://doi.org/10.1016/j.geoderma.2005.04.025, 2006.

Biney, J.K.M., Borůvka, L., Chapman Agyeman, P., Němeček, K. and Klement, A.: Comparison of Field and Laboratory Wet Soil Spectra in the Vis-NIR Range for Soil Organic Carbon Prediction in the Absence of Laboratory Dry Measurements, Remote Sens, 12(18), 3082. https://doi.org/10.3390/rs12183082, 2020

Charrad, M., Ghazzali, N., Boiteau, V., and Niknafs, A.: NbClust: An R Package for Determining the Relevant Number of Clusters in a Data Set. J. Stat. Softw., 61, 1–36. https://doi.org/10.18637/jss.v061.i06, 2014.

Chen, H., Song, Q., Tang, G., Feng, Q., and Lin, L.: The Combined Optimization of Savitzky-Golay Smoothing and Multiplicative Scatter Correction for FT-NIR PLS Models, International Scholarly Research Notices, 2013, 642190. https://doi.org/10.1155/2013/642190, 2013.

Christy, C.D.: Real-time measurement of soil attributes using on-the-go near infrared reflectance spectroscopy, Computers and Electronics in Agriculture, 61(1), 10-19, https://doi.org/10.1016/j.compag.2007.02.010, 2008.

Clark R., and Roush, T.: Reflectance Spectroscopy: Quantitative Analysis Techniques for Remote Sensing Applications, Journal of Geophysical Research, 89(B7), 6329-6340, https://doi.org/198410.1029/JB089iB07p06329, 1984.

https://doi.org/10.5194/egusphere-2022-273
Preprint. Discussion started: 31 May 2022

Colombo, C., Palumbo, G., Di Iorio, E., Sellitto, V.M., Comolli, R., Stellacci, A.M., and Castrignanò, A.: Soil organic carbon variation in Alpine landscape (Northern Italy) as evaluated by diffuse reflectance spectroscopy, Soil Sci Soc Am J, 78, 794-804, https://doi.org/10.2136/sssaj2013.11.0488, 2014.

Conforti, M., Matteucci, G., and Buttafuoco, G.: Using laboratory Vis-NIR spectroscopy for monitoring some forest soil properties, J Soils Sediments, 18, 1009-1019. https://doi.org/10.1007/s11368-017-1766-5, 2018.

Crucil, G., Castaldi, F., Aldana, E., Wesemael, B., and Macdonald, A., Oost, K.: Assessing the Performance of UAS-Compatible Multispectral and Hyperspectral Sensors for Soil Organic Carbon Prediction, Sustainability, 11, https://doi.org/10.3390/su11071889, 2019.

Dalal, R. C., and Henry, R. J.: Simultaneous determination of moisture, organic carbon and total nitrogen by near infrared reflectance spectrophotometry. Soil Science Society of America Journal, 50, 120-123. https://doi.org/10.2136/sssaj1986.03615995005000010023x, 1986.

Daniel, K.W., Tripathi, N.K., Honda, K., and Apisit, E.: Analysis of VNIR (400–1100 nm) spectral signatures for estimation of soil organic matter in tropical soils of Thailand, International Journal of Remote Sensing, 25, 643-652. https://doi.org/10.1080/0143116031000139944, 2004.

Denis, A, Stevens, A., Wesemael, B., Udelhoven, T., and Tychon, B.: Soil organic carbon assessment by field and airborne spectrometry in bare croplands: Accounting for soil surface roughness, Geoderma, 226–227, 94–102. https://doi.org/10.1016/j.geoderma.2014.02.015, 2004.

Dotto, A. Dalmolin, R. Caten, A., and Grunwald, S.: A systematic study on the application of scatter-corrective and spectral-derivative preprocessing for multivariate prediction of soil organic carbon by Vis-NIR spectra, Geoderma, 314, 262-274, https://doi.org/10.1016/j.geoderma.2017.11.006, 2018

Ellinger, M., Merbach, I., Werban, U., and Ließ, M.: Error propagation in spectrometric functions of soil organic carbon, SOIL, 5, 275-288. https://doi.org/10.5194/soil-5-275-2019, 2019.

Filzmoser, P., and Gschwandtner, M.: mvoutlier: Multivariate Outlier. Detection Based on Robust Methods. R package version 2.0.9, https://CRAN.R-project.org/package=mvoutlier, 2018

Ge, Y., Morgan, C.L.S., Grunwald, S., Brown, D.J., and Sarkhot, D.V.: Comparison of soil reflectance spectra and calibration models obtained using multiple spectrometers. Geoderma, 161, 202-211. https://doi.org/10.1016/j.geoderma.2010.12.020, 2011.

Franceschini, M.H.D., Demattê, J.A.M., Kooistra, L., Bartholomeus, H., Rizzo, R., Fongaro, C.T., and Molin, J.P.: Effects of external factors on soil reflectance measured on-the-go and assessment of potential spectral correction through orthogonalisation and standardisation procedures, Soil Tillage Res., 177, 19-36. https://doi.org/10.1016/j.still.2017.10.004, 2018.

Gholizadeh, A; Carmon, N; Klement, A; Ben-Dor, E; Borůvka, L.: Agricultural Soil Spectral Response and Properties Assessment: Effects of Measurement Protocol and Data Mining Technique, Remote Sensing, 9(10), 1078. https://doi.org/10.3390/rs9101078, 2017.

https://doi.org/10.5194/egusphere-2022-273
Preprint. Discussion started: 31 May 2022

Grosse, M., and Hierold, W.: Long-term Field Experiments in Germany (Version 1.0). BonaResData Centre, Leibniz Centre for Agricultural Landscape Research (ZALF), https://doi.org/10.20387/BONARES-3TR6-MG8R, 2019

Grosse, M., Hierold, W., Ahlborn, M.C., Piepho, H-P., and Helming, K.: Long-term field experiments in Germany: classification and spatial representation, SOIL, 6, 579-596, https://doi.org/10.5194/soil-6-579-2020, 2020.

Guio Blanco, C. M., Brito Gomez, V. M., Crespo, P., and Ließ, M.: Spatial prediction of soil water retention in a Páramo landscape: Methodological insight into machine learning using random forest, Geoderma, 316, 100-114. https://doi.org/10.1016/j.geoderma.2017.12.002. 2018.

Ji, W., Viscarra Rossel, R. A., and Shi, Z.: Improved estimates of organic carbon using proximally sensed vis–NIR spectra corrected by piecewise direct standardization. European Journal of Soil Science, 66(4), 670-678, https://doi.org/10.1111/ejss.12271, 2015a.

Ji, W., Viscarra Rossel, R. A., and Shi, Z.: Accounting for the effects of water and the environment on proximally sensed vis–NIR soil spectra and their calibrations, European Journal of Soil Science, 66(3), 555-565, https://doi.org/10.1111/ejss.12239, 2015b.

Ji, W., Li, S., Chen, S., Shi, Z., Viscarra Rossel, R.A., and Mouazen, A.M.: Prediction of soil attributes using the Chinese soil spectral library and standardized spectra recorded at field conditions, Soil and Tillage Research, 155, 492-500. https://doi.org/10.1016/j.still.2015.06.004, 2016.

Jiang, Q., Chen, Y., Guo, L., Fei, T., and Qi, K.: Estimating Soil Organic Carbon of Cropland Soil at Different Levels of Soil Moisture Using VIS-NIR Spectroscopy, Remote Sens., 8, 755, https://doi.org/10.3390/rs8090755, 2016.

Hopkins, D.W. NIR news, 14(5), 10, 2003.

Kawamura, K., Tsujimoto, Y., Rabenarivo, M., Asai, H., Andriamananjara, A., and Rakotoson, T.: Vis-NIR Spectroscopy and PLS Regression with Waveband Selection for Estimating the Total C and N of Paddy Soils in Madagascar, Remote Sensing, 9, https://doi.org/10.3390/rs9101081, 2017.

Kawamura, K., Nishigaki, T., Tsujimoto, Y., Andriamananjara, A., Rabenaribo, M., Asai, H., Rakotoson, T., and Razafimbelo, T.: Exploring relevant wavelength regions for estimating soil total carbon contents of rice fields in Madagascar from Vis-NIR spectra with sequential application of backward interval PLS, Plant Production Science, 24(1), 1-14. https://doi.org/10.1080/1343943X.2020.1785898, 2021.

Knox, N.M., Grunwald, S., McDowell, M.L., Bruland, G.L., Myers D.B., and Harris, W.G.: Modelling soil carbon fractions with Visible Near-Infrared (VNIR) and Mid-Infrared (MIR) spectroscopy, Geoderma, 239-240, 229-239. https://doi.org/10.1016/j.geoderma.2014.10.019, 2015.

Körschens, M. and Pfefferkorn, A.: Bad Lauchstädt – The Static Fertilization Experiment and other Long-Term Field Experiments.UFZ – Umweltforschungszentrum: Leipzig-Halle GmbH, Germany, 1998.

Körschens, M.: The importance of long-term field experiments for soil science and environmental research - A review, Plant, Soil and Environment, 52, 1-8, 2006.

https://doi.org/10.5194/egusphere-2022-273
Preprint. Discussion started: 31 May 2022

Kuhn, M., and Johnson, K.: Applied Predictive Modeling, Springer, New York, USA, https://doi.org/10.1007/978-1-4614-6849-3, 2013.

Martens, H., Jensen, S.A., and Geladi, P.: Multivariate linearity transformations for near infrared reflectance spectroscopy, in: O.H.J. Christie (Ed.), Proc. Nordic Symp. Applied Statistics (pp. 205-234), Stokkland, Forlag: Stavanger, Norway. 1983.

Lin, L.: A concordance correlation coefficient to evaluate reproducibility, Biometrics, 45, 255-268. https://doi.org/10.2307/2532051, 1989.

Mehmood, T., Liland, K., Snipen, L., and Sæbø, S.: A review of variable selection methods in Partial Least Squares Regression, Chemometrics and Intelligent Laboratory Systems, 118, 62-69, https://doi.org/10.1016/j.chemolab.2012.07.010, 2012.

Merbach, I. and Schulz, E.: Long-term fertilization effects on crop yields, soil fertility and sustainability in the Static Fertilization Experiment Bad Lauchstädt under climatic conditions 2001–2010, Arch. Agron. Soil Sci., 59, 1041-1057, https://doi.org/10.1080/03650340.2012.702895, 2013.

Mevik, B., Wehrens, R., and Liland, K.: pls: Partial Least Squares and Principal Component Regression. R package version 2.7-2., https://CRAN.R-project.org/package=pls, 2019

Minasny, B., McBratney, A.B., Bellon-Maurel, V., Roger, J.M., Gobrecht A., Ferrand, L., and Joalland S.: Removing the effect of soil moisture from nir diffuse reflectance spectra for the prediction of soil organic carbon, Geoderma, 167-168, 118-124. https://doi.org/10.1016/j.geoderma.2011.09.008, 2011.

Minasny, B., Malone, B. P., McBratney, A. B., Angers, D. A., Arrouays, D., Chambers, A., … and Field, D.J.: Soil carbon 4 per mille, Geoderma, 292, 59-86. https://doi.org/10.1016/j.geoderma.2017.01.002, 2017.

Nawar, S., Munnaf, M. A., and Mouazen, A.: Machine learning based on-line prediction of soil organic carbon after removal of soil moisture effect, Remote Sensing, 12(8), https://doi.org/10.3390/rs12081308, 2020.

Nocita, M., Stevens, A., Noon, C., and Van Wesemael, B.: Prediction of soil organic carbon for different levels of soil moisture using Vis-NIR spectroscopy, Geoderma, 199, 37-42. https://doi.org/10.1016/j.geoderma.2012.07.020, 2012.

Lal, R. Soil carbon sequestration to mitigate climate change, Geoderma, 123, 1-22, https://doi.org/10.1016/j.geoderma.2004.01.032, 2004.

Ladoni, M., Bahrami, H.A., Alavipanah, S.K., and Norouzi, A.: Estimating soil organic carbon from soil reflectance: A review, Precision Agriculture, 11, 82-99, https://doi.org/10.1007/s11119-009-9123-3, 2010.

Le S., Josse, J., Husson, F.: FactoMineR: An R Package for Multivariate Analysis. Journal of Statistical Software, 25(1), 1-18. https://doi.org/10.18637/jss.v025.i01, 2008.

Lee, K.S., Lee, D.H., Sudduth, K.A., Chung, S.O., Kitchen, N.R., Drummond, S.T.: Wavelength identification and diffuse reflectance estimation for surface and profile soil properties, Trans. ASABE, 52(3), 683-695, https://doi.org/10.13031/2013.27385, 2009.

Liu, Y., Zhou, S., Zhang, G., Chen, Y., Li, S., Hong, Y., Shi, T., Wang, J., and Liu, Y.: Application of spectrally derived soil type as ancillary data to improve the estimation of soil organic carbon by using the Chinese soil Vis-NIR spectral library, Remote Sens., 10, 1-16. https://doi.org/10.3390/rs10111747, 2018.

https://doi.org/10.5194/egusphere-2022-273
Preprint. Discussion started: 31 May 2022

Palacio-Orueta, A., and Ustin, S.L.: Remote sensing of soil properties in the Santa Monica mountains I. Spectral analysis, Remote Sensing of Environment, 65, 170-183, https://doi.org/10.1016/S0034-4257(98)00024-8, 1998.

Peng, X, Shi, T., Song, A., Chen, Y., and Gao, W.: Estimating soil organic carbon using VIS/NIR spectroscopy with SVMR and SPA methods. Remote Sensing 6(4), 2699-2717. https://doi.org/10.3390/rs6042699, 2014.

Pimstein, A., Notesco, G., and Ben-Dor, E.: Performance of Three Identical Spectrometers in Retrieving Soil Reflectance under Laboratory Conditions, Soil Sci. Soc. Am. J., 75, 746-759, https://doi.org/10.2136/sssaj2010.0174, 2011.

Peng, Y., Xiong, X., Adhikari, K., Knadel, M., Grunwald, S., and Greve, M.H.: Modeling soil organic carbon at regional scale by combining multi-spectral images with laboratory spectra, PLoS ONE, 10(11), 1-22. https://doi.org/10.1371/journal.pone.0142295, 2015.

Poulton, P., Johnston, J., Macdonald, A., White, R., and Powlson, D.: Major limitations to achieving "4 per 1000" increases in soil organic carbon stock in temperate regions: Evidence from long-term experiments at Rothamsted Research, United Kingdom, Glob Change Biol., 24, 2563- 2584. https://doi.org/10.1111/gcb.14066, 2018.

Reeves III, J.B.: Near- versus mid-infrared diffuse reflectance spectroscopy for soil analysis emphasizing carbon and laboratory versus on-site analysis: where are we and what needs to be done?, Geoderma, 158(1-2), 3-14. https://doi.org/10.1016/j.geoderma.2009.04.005, 2010.

Rienzi, E.A., Mijatovic, B., Mueller, T.G., Matocha, C.J., Sikora, F.J., and Castrignanò, A.: Prediction of soil organic carbon under varying moisture levels using reflectance spectroscopy, Soil Sci. Soc. Am. J., 78, 958-967. https://doi.org/10.2136/sssaj2013.09.0408, 2014.

Rinnan, A., Berg, F., and Engelsen, S.: Review of the Most Common pre-Processing Techniques for Near-Infrared Spectra, Trends in Analytical Chemistry, 28, 1201-1222, https://doi.org/10.1016/j.trac.2009.07.007, 2009.

Roudier, P., Hedley, C.B., Lobsey, C.R., Rossel, R.V., and Leroux, C.: Evaluation of two methods to eliminate the effect of water from soil vis–NIR spectra for predictions of organic carbon, Geoderma, 296, 98-107, https://doi.org/10.1016/j.geoderma.2017.02.014, 2017.

Roudier, P.: spectacles: Storing and Manipulating Spectroscopy Data in R, R package version 0.5-2-2. https://CRAN.R-project.org/package=spectacles, 2020

Roger, J.M.; Chauchard, F.; Bellon-Maurel, V.: EPO-PLS external parameter orthogonalisation of PLS application to temperature-independent measurement of sugar content of intact fruits, Chemom. Intell. Lab. Syst., 66, 191–204, 2003.

Sarathjith, M.C., Das, B. S., Wani, S. P., and Sahrawat, K.L.: Variable indicators for optimum wavelength selection in diffuse reflectance spectroscopy of soils, Geoderma, 267, 1-9, https://doi.org/10.1016/j.geoderma.2015.12.031, 2016.

Savitzky, A., and Golay, M.: Smoothing and differentiation of data by simplified least squares procedures, Anal. Chem. 36(8), 1627-1639, https://doi.org/10.1021/ac60214a047, 1964.

Seidel, M., Hutengs, C., Ludwig, B., Thiele-Bruhn, S., and Vohland, M.: Strategies for the efficient estimation of soil organic carbon at the field scale with vis-NIR spectroscopy: Spectral libraries and spiking vs. local calibrations, Geoderma, 354, 113856. https://doi.org/10.1016/j.geoderma.2019.07.014, 2019.

https://doi.org/10.5194/egusphere-2022-273
Preprint. Discussion started: 31 May 2022

Soriano-Disla, J., Janik, LJ., Viscarra Rossel, R.A., Macdonald, LM., and McLaughlin M.J.: The Performance of Visible, Near-, and Mid-Infrared Reflectance Spectroscopy for Prediction of Soil Physical, Chemical, and Biological Properties, Applied Spectroscopy Reviews, 49, 2, 139-186. https://doi.org/10.1080/05704928.2013.811081, 2014.

Stevens, A., Wesemael, B., Bartholomeus, H., Rosillon, D., Tychon, B., and Ben-Dor, E.: Laboratory, Field and Airborne Spectroscopy for Monitoring Organic Carbon Content in Agricultural Soils, Geoderma, 144, 395-404. https://doi.org/10.1016/j.geoderma.2007.12.009, 2008.

Stevens A., and Ramirez-Lopez, L.: An introduction to the prospectr package R package Vignette, R package version 0.1.3, https://CRAN.R-project.org/package=prospectr, 2014.

Stenberg, B., Viscarra Rossel, R.A., Mouazen, A.M., and Wetterlind, J.: Visible and near infrared spectroscopy in soil science, Adv. Agron., 107, 163-215. https://doi.org/10.1016/S0065-2113(10)07005-7, 2010.

Sudduth, K.A., and Hummel, J.W.: Evaluation of reflectance methods for soil and soil organic matter sensing,Transactions of the ASAEI, 34, 1900-1909. . https://doi.org/10.13031/2013.31816, 1991.

Shepherd, K.D., and Walsh, M.G.: Development of reflectance spectral libraries for characterization of soil properties, Soil Science Society of America Journal, 66, 988-998, https://doi.org/10.2136/sssaj2002.9880, 2002.

United Nations / Framework Convention on Climate Change: Adoption of the Paris Agreement, 21st Conference of the Parties, Paris: United Nations, https://unfccc.int/resource/docs/2015/cop21/eng/l09r01.pdf, 2015.

Vasques, G.M., Grunwald, S., and Sickman, J.O.: Modeling of soil organic carbon fractions using visible/near-infrared spectroscopy. Soil Sci. Soc. Am. J. 73, (1), 176-184. https://doi.org/10.2136/sssaj2002.9880, 2009.

Viscarra Rossel, R.A., Walvoort, D.J.J., McBratney, A.B., Janik, L.J., and Skjemsta, J.O.: Visible, near infrared, mid infrared or combined diffuse reflectance spectroscopy for simultaneous assessment of various soil properties, Geoderma, 131, 59-75. https://doi.org/10.1016/j.geoderma.2005.03.007, 2006.

Viscarra Rossel, R., Fouad, Y., and Walter, C.: Using a digital camera to measure soil organic carbon and iron contents, Biosystems Engineering, 100, 149-159. https://doi.org/10.1016/j.biosystemseng.2008.02.007, 2008.

Viscarra Rossel, R.A., Cattle, S.R., Ortega, A., and Fouad, Y.: In situ measurements of soil colour, mineral composition and clay content by vis-NIR spectroscopy, Geoderma, 150, 253-266. https://doi.org/10.1016/j.geoderma.2009.01.025, 2009.

Wang, Y., Veltkamp, D.J., and Kowalski, B.R.: Multivariate Instrument Standardization, Anal. Chem, 63, 2750–2756, 1991.

Wang C.K., and Pan, X.Z.: Estimation of clay and soil organic carbon using visible and near-infrared spectroscopy and unground samples. Soil Sci. Soc. Am., 80, 1393-1402. https://doi.org/10.2136/sssaj2016.05.0136, 2016.

West, T.O., and Marland, G.: A synthesis of carbon sequestration, carbon emissions, and net carbon flux in agriculture: Comparing tillage practices in the United States. Agric. Ecosyst. Environ. 91, 217-232. https://doi.org/10.1016/S0167-8809(01)00233-X, 2002.

Wickham, H.: ggplot2: Elegant Graphics for Data Analysis, Springer-Verlag, New York, USA, 2016.

Wijewardane, N.K., Hetrick, S., Ackerson, J., Morgan, C.L.S., and Ge, Y.: VisNIR integrated multi-sensing penetrometer for in situ high-resolution vertical soil sensing. Soil Tillage Res. 199, 104604, https://doi.org/10.1016/j.still.2020.104604, 2020.

https://doi.org/10.5194/egusphere-2022-273
Preprint. Discussion started: 31 May 2022

570 Wold, S, Sjostrom, M, and Eriksson, L.: PLS-Regression: a Basic Tool of Chemometrics, Chemom. Intell. Lab. Syst., 58:109-130, https://doi.org/10.1016/S0169-7439(01)00155-1, 2001.

Wold, S., Johansson, A., and Cochi, M. PLS - Partial Least-Squares Projections to Latent Structures, in: 3D QSAR in Drug Design, Theory Methods and Applications, edited by: Kubinyi H., ESCOM Science Publishers, Leiden, 523-550, 1993.

Yang, H., Kuang, B., and Mouazen, A.M.: Quantitative analysis of soil nitrogen and carbon at a farm scale using visible and
575 near infrared spectroscopy coupled with wavelength reduction, Eur. J. Soil Sci., 63, 410-420. https://doi.org/10.1111/j.1365-2389.2012.01443.x, 2012

Zhou, S., Wenjun, J., Viscarra Rossel, R., Chen, S., and Zhou, Y.: Prediction of soil organic matter using a spatially constrained local partial least squares regression and the Chinese vis-NIR spectral library: vis-NIR predictions of soil carbon with scL-PLSR, European Journal of Soil Science, 66, 410-420, https://doi.org/10.1111/ejss.12272, 2015.

https://doi.org/10.5194/egusphere-2022-273
Preprint. Discussion started: 31 May 2022

Tables

Table 1 Preprocessing methods and corresponding wavelength ranges.

Preprocessing method	ASD wavelength range	Veris wavelength range	Abbreviation
Savitsky-Golay	405-2195	432-2201	SG
Saviztky-Golay w=11 and continuum removal	405-2195	432-2201	SGCR
Gap segment algorithm (w=11, s=10)	415-2185	408-2186	gapDer
Multiplicative scatter correction	400-2200	403-2201	MSC

w = window size, s = segment size

Table 2 Optimal parameter values of PDS and EPO used for model building.

	Veris			ASD		
	PDS		EPO	PDS		EPO
	ncomp	w	ncomp	ncomp	w	ncomp
SG	1	2	7	4	5	9
SGCR	2	4	5	5	8	8
gapDer	1	2	5	3	3	8
MSC	1	2	6	2	9	9

SG: Saviztky Golay, SGCR: Saviztky Golay + continuum removal, gapDer: gap segment algorithm (gapDer), MSC: multiplicative scatter correction, ncomp: number of components, w: windows size, PDS: Piecewise Direct Standardization. EPO: External Parameter Orthogonalization.

https://doi.org/10.5194/egusphere-2022-273
Preprint. Discussion started: 31 May 2022

Table 3 Comparison of wavelength local maxima peak matches between ASD laboratory MSC and close peaks (±10 nm for ASD and ±20 nm for Veris) from the other datasets regarding variable importance in projection. SG: Saviztky Golay, SGCR: Saviztky Golay + continuum removal, gapDer: gap segment algorithm, MSC: multiplicative scatter correction.

ASD laboratory MSC	Veris laboratory				Veris field				ASD laboratory		
Wavelength (nm)	SG	SGCR	gapDer	MSC	SG	SGCR	gapDer	MSC	SG	SGCR	gapDer
557		x				x	x			x	x
909						x	x				
1045											x
1111									x	x	
1196				x	x	x		x	x		x
1272								x	x		
1330	x	x		x		x			x	x	
1412	x	x	x	x	x	x		x	x	x	x
1488		x		x	x			x	x	x	
1621	x			x	x	x			x	x	x
1729	x	x		x	x			x	x		
1784			x	x			x		x		x
1907	x	x	x	x	x	x		x			x
2008								x	x		
2142	x			x					x		
Total matches	6	6	3	9	6	7	3	7	11	6	7

https://doi.org/10.5194/egusphere-2022-273
Preprint. Discussion started: 31 May 2022

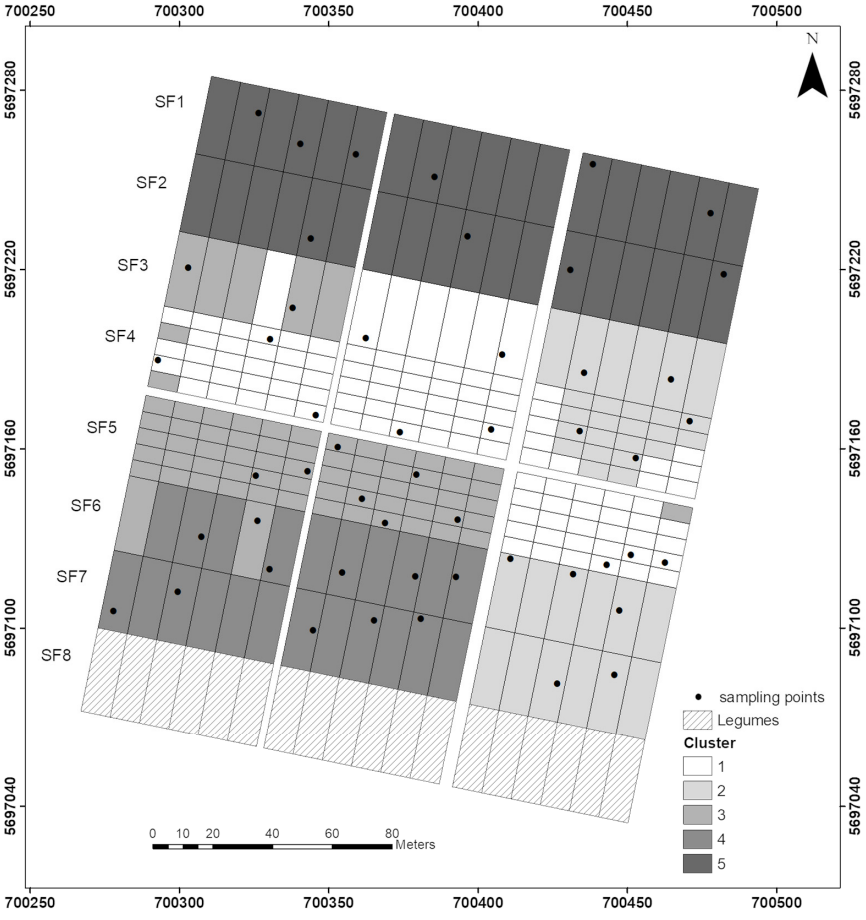

Figure 1: Study area located in Bad Lauchstädt. SF: subfield number. Sampling points were selected by stratified random sampling. Coordinate reference system: EPSG 25833.

https://doi.org/10.5194/egusphere-2022-273
Preprint. Discussion started: 31 May 2022

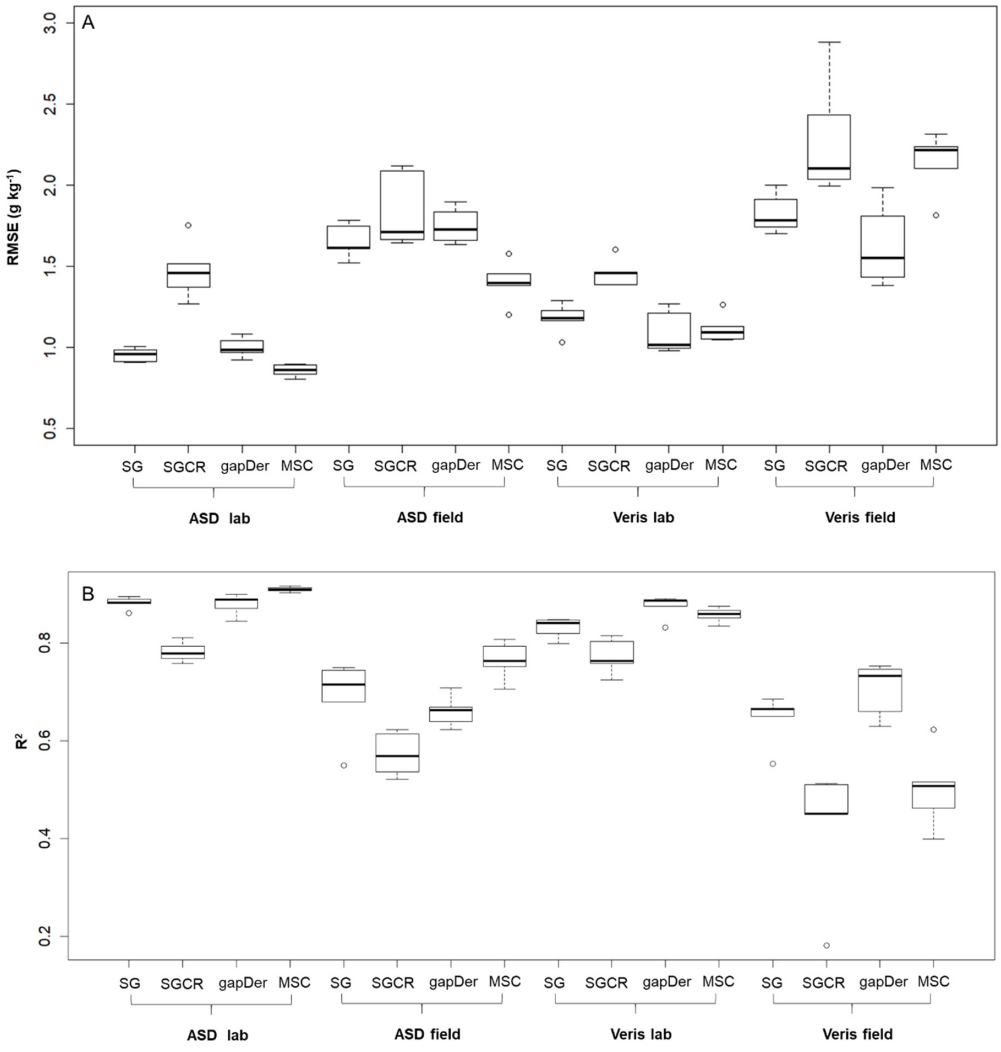

Figure 2: Predictive model performance of all 16 datasets (5 values per boxplot). A: Root mean square error (RMSE) and B: R squared (R^2). SG: Saviztky Golay, SGCR: Saviztky Golay + continuum removal, gapDer: gap segment algorithm (gapDer), MSC: multiplicative scatter correction.

610

https://doi.org/10.5194/egusphere-2022-273
Preprint. Discussion started: 31 May 2022

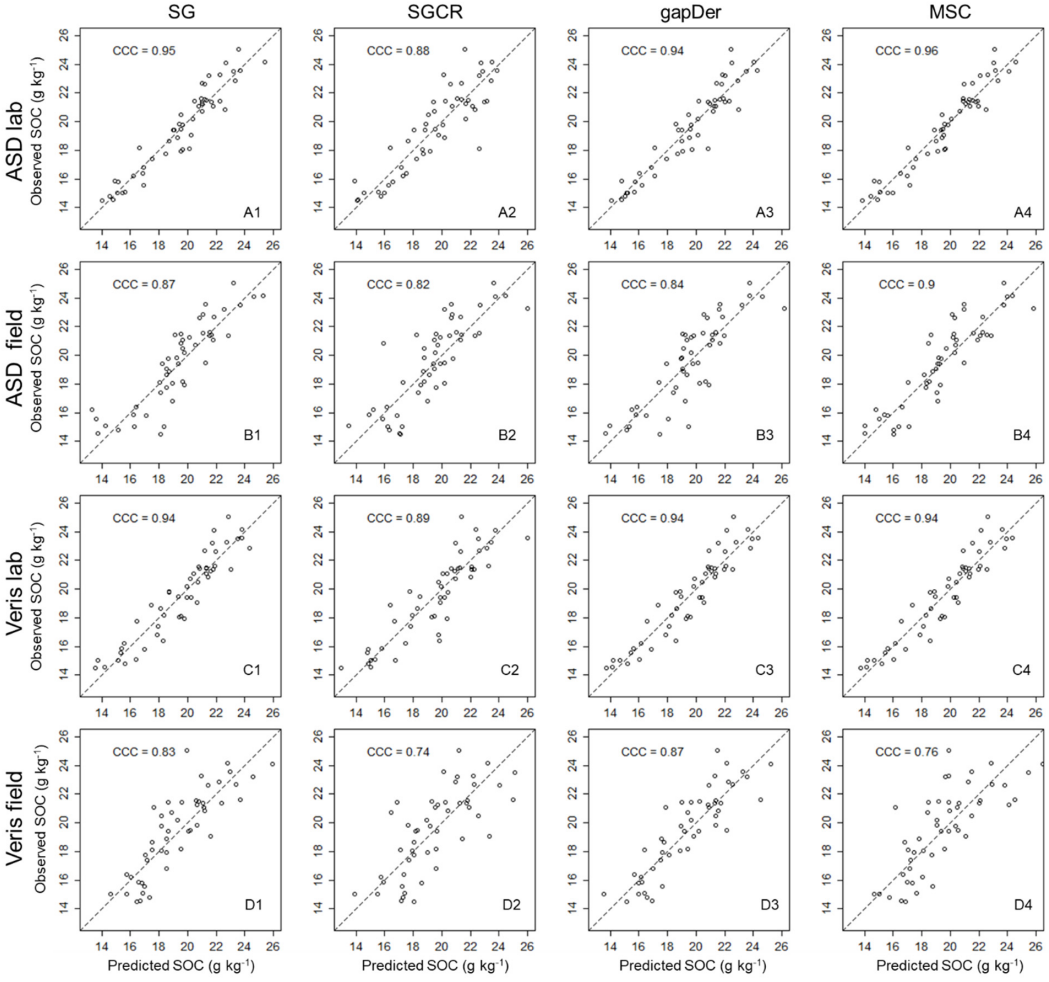

Figure 3: Predicted versus observed values for the 16 datasets (average of 5 predictions). CCC: concordance correlation coefficient. SG: Saviztky Golay, SGCR: Saviztky Golay + continuum removal, gapDer: gap segment algorithm, MSC: multiplicative scatter correction.

https://doi.org/10.5194/egusphere-2022-273
Preprint. Discussion started: 31 May 2022

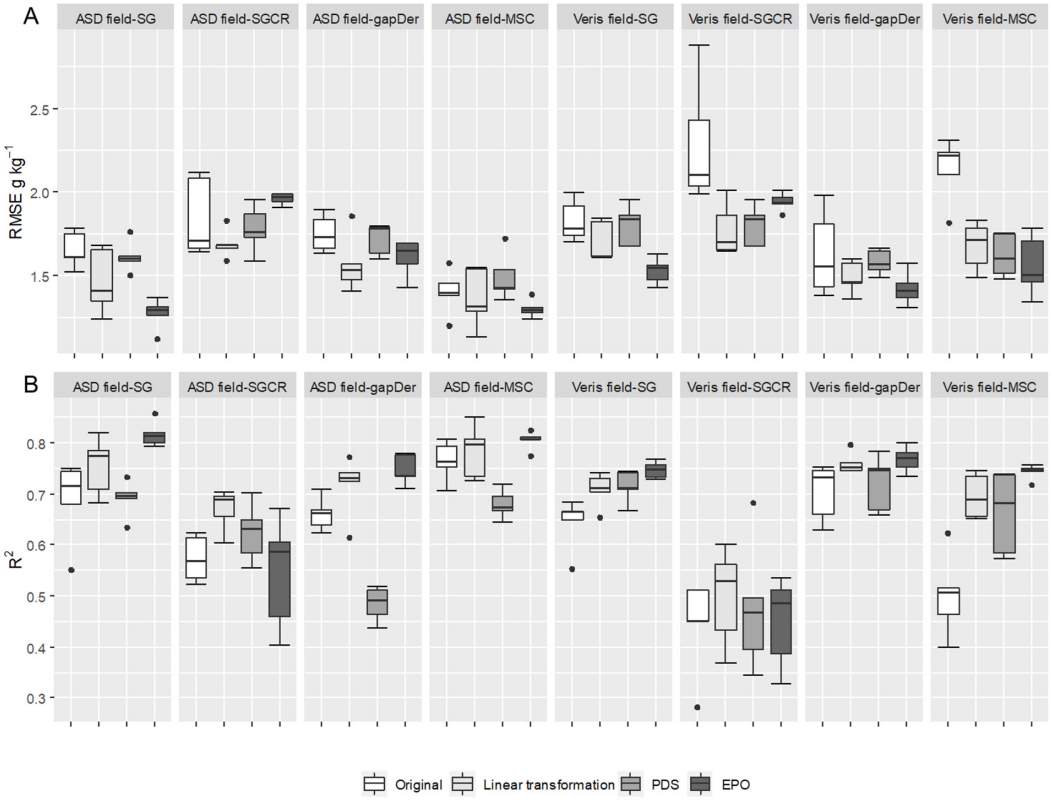

Figure 4: Predictive model performance of the 8 field datasets before and after spectral correction (5 values per boxplot). A: Root mean square error (RMSE) and B: R squared (R^2) of the model prediction. SG: Saviztky Golay, SGCR: Saviztky Golay + continuum removal, gapDer: gap segment algorithm, MSC: multiplicative scatter correction. PDS: Piecewise Direct Standardization. EPO: External Parameter Orthogonalization.

https://doi.org/10.5194/egusphere-2022-273
Preprint. Discussion started: 31 May 2022

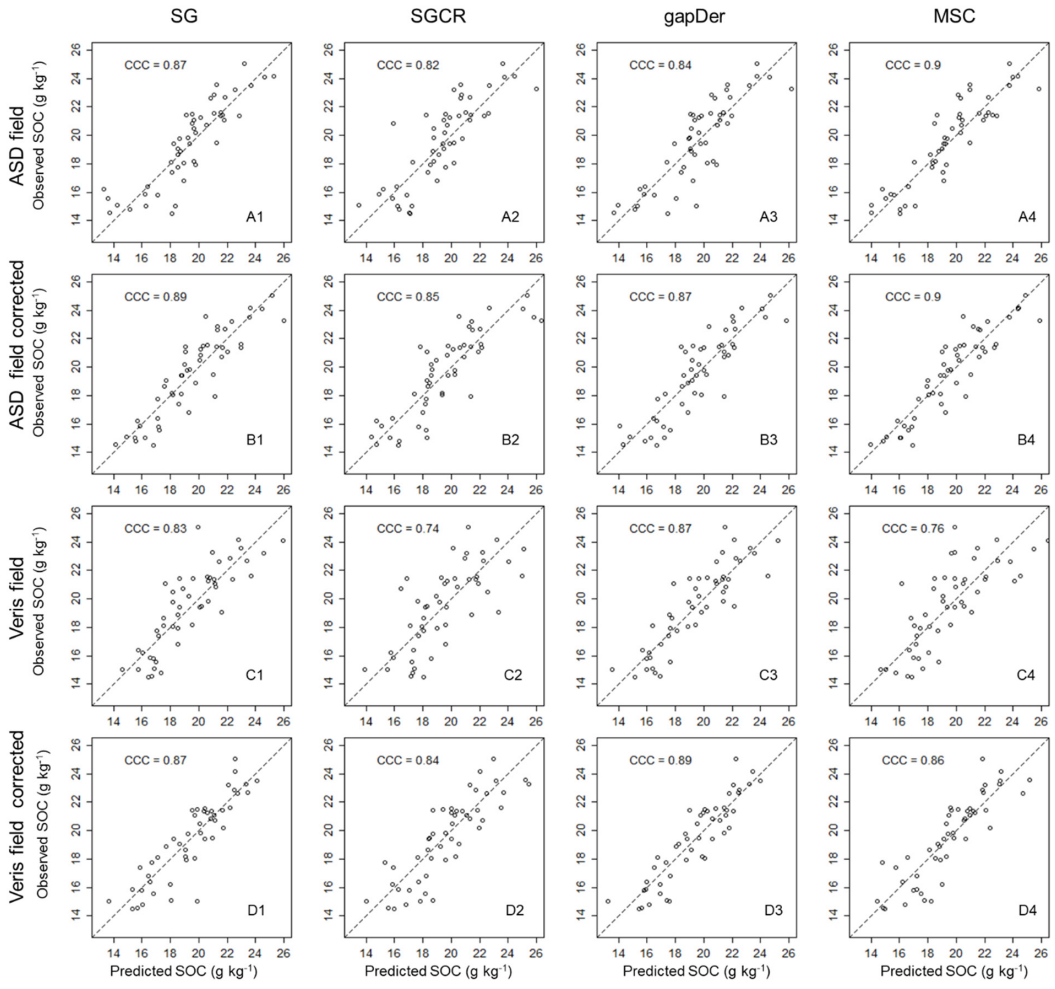

Figure 5: Predicted versus observed values comparing ASD and Veris field data before spectral correction and the best results after the data correction (average of 5 predictions). CCC: concordance correlation coefficient. SG: Saviztky Golay, SGCR: Saviztky Golay + continuum removal, gapDer: gap segment algorithm, MSC: multiplicative scatter correction.

https://doi.org/10.5194/egusphere-2022-273
Preprint. Discussion started: 31 May 2022

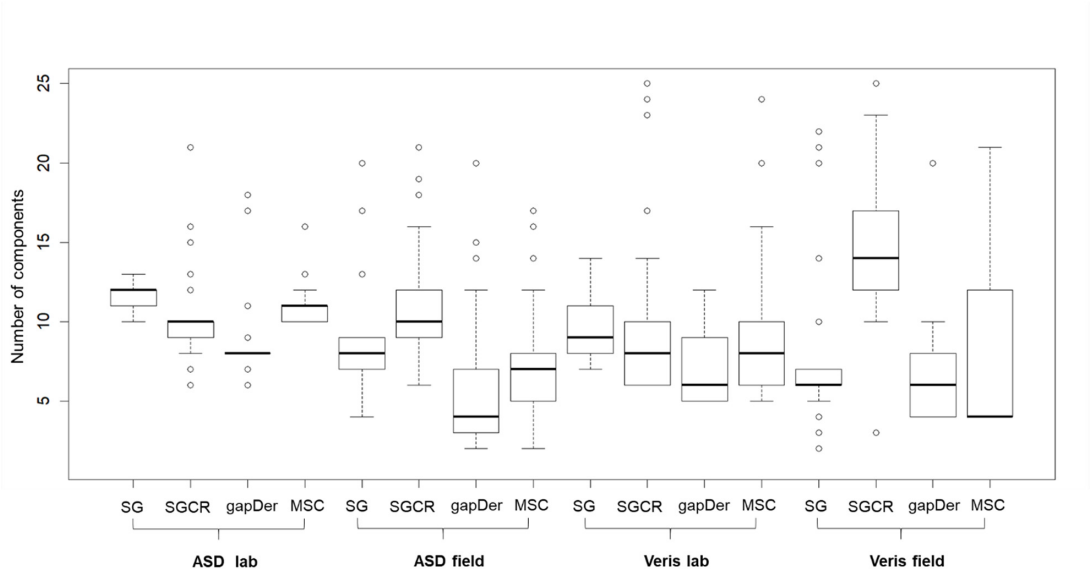

630 **Figure 6:** Boxplots of the tuned number of components of the 25 PLSR models built from each of the 16 datasets. SG: Saviztky Golay, SGCR: Saviztky Golay + continuum removal, gapDer: gap segment algorithm, MSC: multiplicative scatter correction.

https://doi.org/10.5194/egusphere-2022-273
Preprint. Discussion started: 31 May 2022

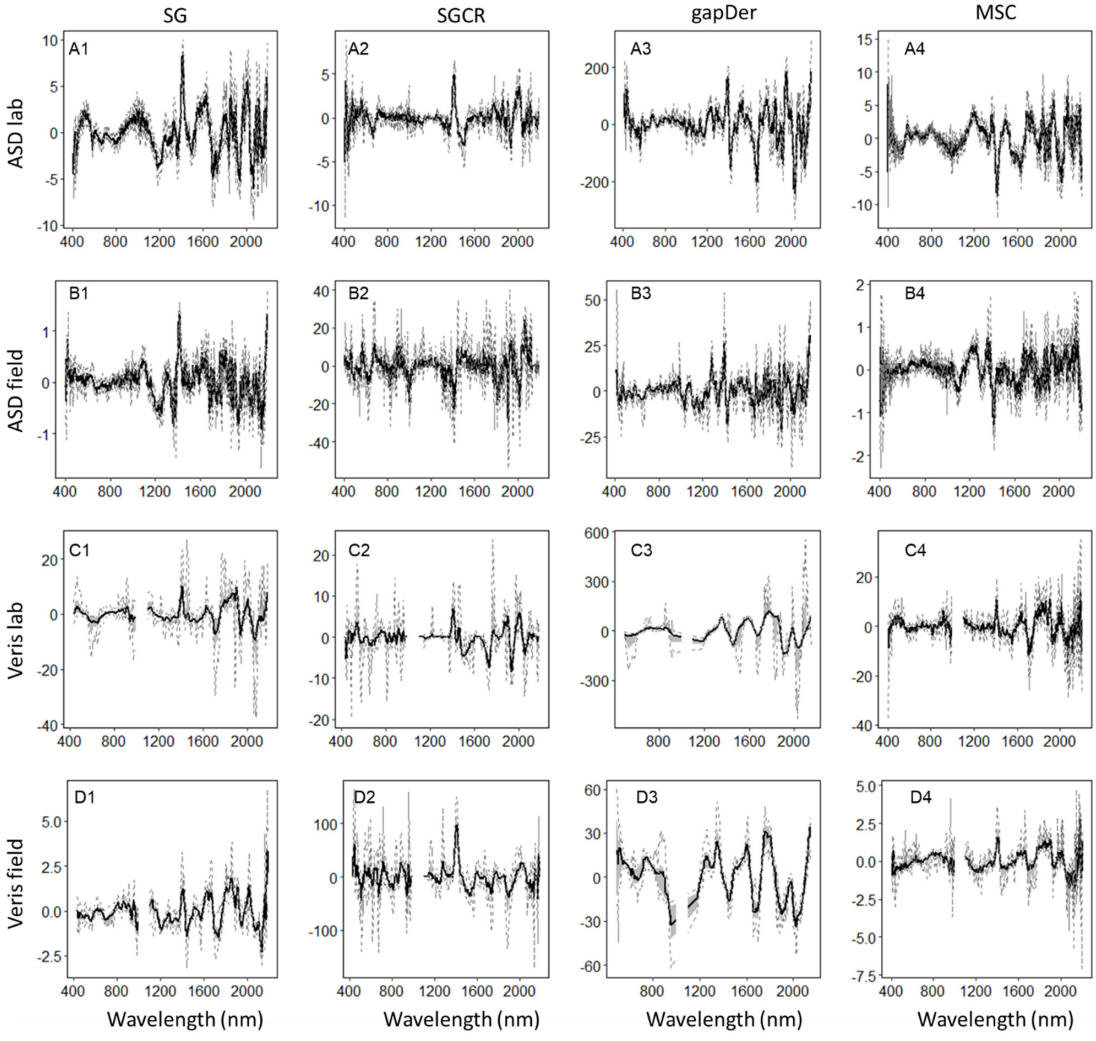

Figure 7: Regression coefficients from 25 models for each dataset. The black line is the median, the gray area shows the interquartile range, and the dashed lines represent the minimum and maximum values. SG: Saviztky Golay, SGCR: Saviztky Golay + continuum removal, gapDer: gap segment algorithm, MSC: multiplicative scatter correction.

https://doi.org/10.5194/egusphere-2022-273
Preprint. Discussion started: 31 May 2022

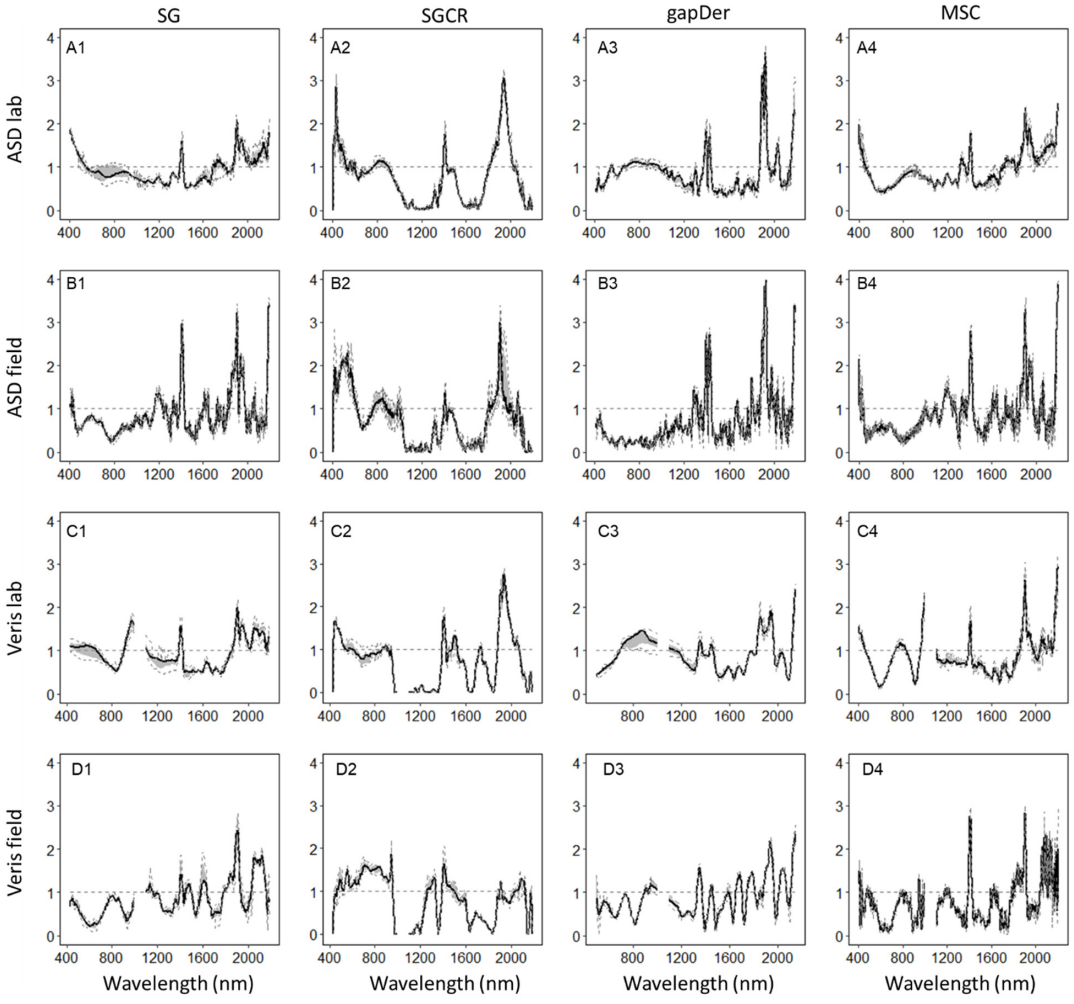

Figure 8: Variable importance in projection from 25 models for each dataset. The black line is the median, the gray area shows the interquartile range, and the dashed lines represent the minimum and maximum values. SG: Saviztky Golay, SGCR: Saviztky Golay + continuum removal, gapDer: gap segment algorithm, MSC: multiplicative scatter correction.

https://doi.org/10.5194/egusphere-2022-273
Preprint. Discussion started: 31 May 2022

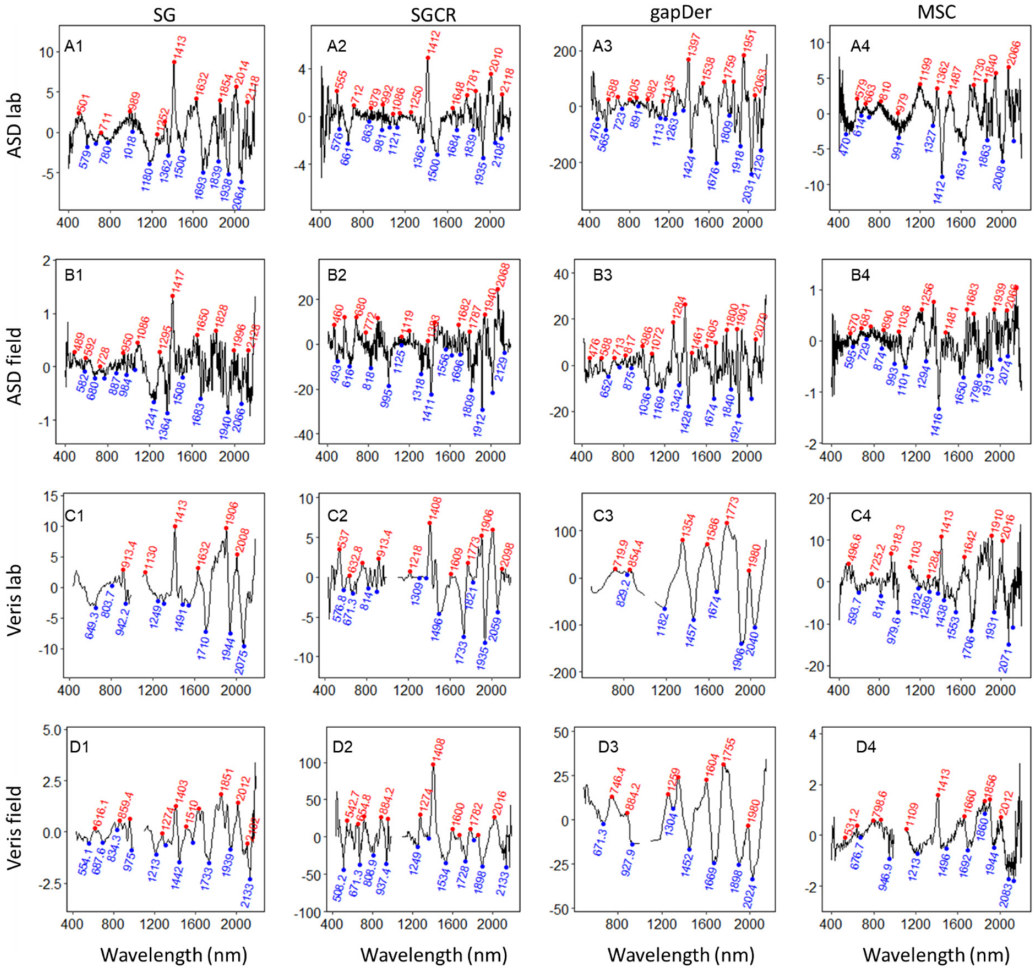

Figure 9: Median local maxima and minima values of regression coefficients for each dataset. SG: Saviztky Golay, SGCR: Saviztky Golay + continuum removal, gapDer: gap segment algorithm, MSC: multiplicative scatter correction.

645

https://doi.org/10.5194/egusphere-2022-273
Preprint. Discussion started: 31 May 2022

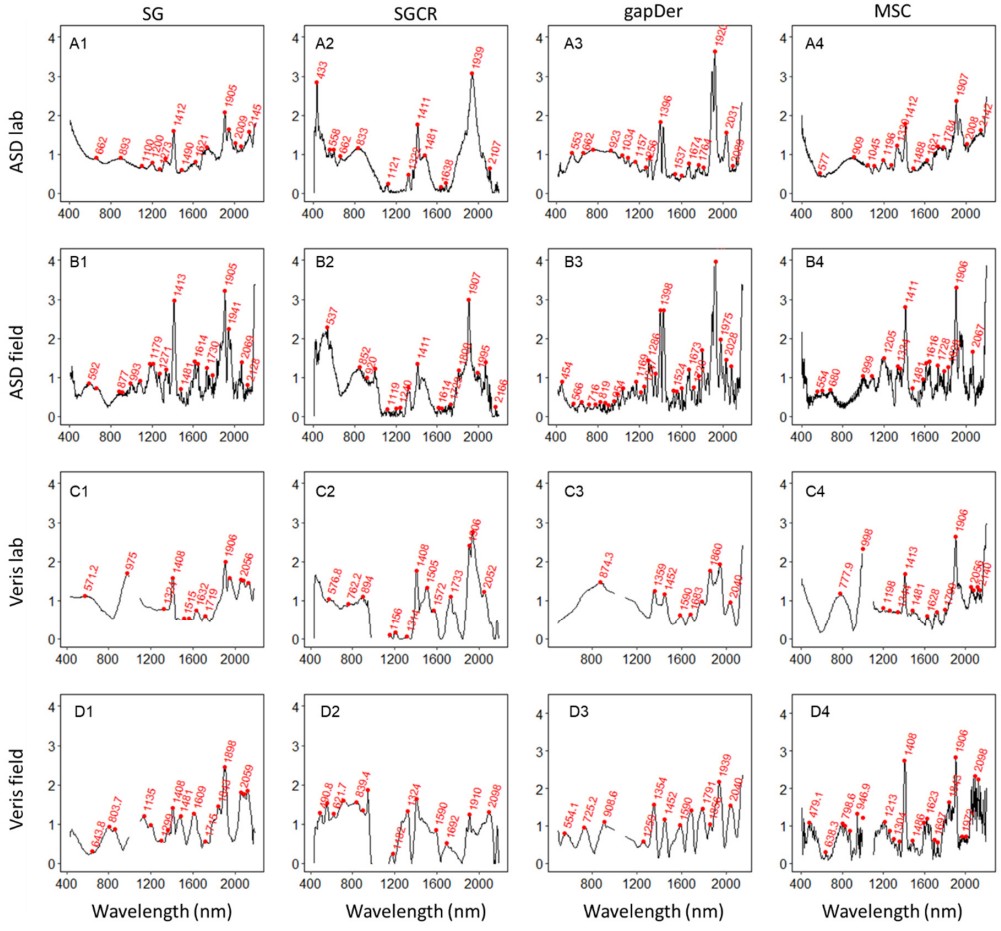

Figure 10: Median local maxima values of Variable importance in projection for each dataset. SG: Saviztky Golay, SGCR: Saviztky Golay + continuum removal, gapDer: gap segment algorithm, MSC: multiplicative scatter correction.

650